Article

Fault Location in Power Electrical Traction Line System

Yimin Zhou [1,2]**, Guoqing Xu** [3,4]**,* and Yanfeng Chen** [1,2]

[1] Shenzhen Institutes of Advanced Technology, Chinese Academy of Sciences, Shenzhen 518055, China; E-Mails: ym.zhou@siat.ac.cn (Y.Z.); yf.chen@siat.ac.cn (Y.C.)

[2] Shenzhen Key Laboratory of Electric Vehicle Powertain Platform and Safety Technology, Shenzhen 518055, China

[3] Department of Electrical Engineering, School of Electronics and Information, Tongji University, No. 4800 Caoan Road, Shanghai 201804, China

[4] Department of Mechanical and Automation Engineering, The Chinese University of Hong Kong, Shatin, Hong Kong

* Author to whom correspondence should be addressed; E-Mail: gq.xu@siat.ac.cn; Tel.: +86-0755-86392189; Fax: +86-0755-86392194.

Abstract: In this paper, methods of fault location are discussed in electrical traction single-end direct power supply network systems. Based on the distributed parameter model of the system, the position of the short-circuit fault can be located with the aid of the current and voltage value at the measurement end of the electrical traction line. Furthermore, the influence of the transient resistance, the position of the locomotive, locomotive load for fault location are also discussed. MATLAB simulation tool is used for the simulation experiments. Simulation results are proved the effectiveness of the proposed algorithms.

Keywords: fault location; traction system; steady-state; resistance analysis

1. Introduction

There is a great interest in precise fault location in electrical traction network systems, which plays an important role in the railway operation due to the consideration of safety, reliability, stability and economy [1,2]. As for a special branch in power system, the characteristics of the power supply structure, operational mode and traction load in the traction system complicate the fault distance measurement

greatly. The more accuracy of the fault is located, the quicker and easier the system is restored. It can lessen the fault patrolling load, decrease stop time for maintenance, reduce customers complaints and improve protection performance.

There is considerable research achievement in the area of fault distance measurement in the transmission and distribution line (including cable) of the power system. Normally, fault can be classified into wire short-circuit fault, contact network cut-line grounding fault and different-phase short-circuit fault, where wire short-circuit fault happens most of the time.

As for single-end direct power supply traction system, the fault is mainly embodied as contact network grounding phenomenon. When fault occurs, there is a transient resistance generated between the fault point and ground. It is a random variable and has no relationship to the distance of the fault point, which is decided by the grounding resistance and the arc resistance generated during the short-circuit period. The short-circuit reactance is normally influenced by the wire material, space structure, ground dirt material conductivity. After the contact network has been constructed, the basic line reactance is determined, which will not be influenced by the ways of short-circuit and power supply.

Methods of fault location can be divided into active and passive two ways. As for active pattern, the fault position is located via injecting particular signal to the system without interrupting the power supply, such as S signal injection approach. However, if intermittent electric-arc phenomena exists at the connection ground point, the injection signal can not be continuous in the electrical line, which can bring more difficulties for the precise fault location. If the fault point is located off-line, extra direct current high voltage should be added to keep the shooting status at the ground position, which would increase cost and complicity of the detection procedure.

On the other hand, passive fault location is achieved via the collected signals of the measurement terminals at the fault occurrence time without the aid of additional equipment. It can be easily applied on the spot. Therefore, passive fault location method is the fault location development direction in distribution power network, such as impedance method [3–6] and traveling wave method [7–9]. Based on the information sources from the measurement point of view, the algorithms of fault location can be divided into single-terminal and double-terminal approaches [10,11].

The theory of impedance for fault distance measurement [12,13] is to calculate the fault loop impedance or reactance under different fault type conditions, which is proportional to the distance between the measurement point and fault point [14]. Through the value from the calculated impedance/reactance at the measurement point divided by the per-unit-length resistance/reactance, the distance from the measurement point to the fault point is acquired [6,15]. In the current fault distance measurement equipment, this method is adopted broadly because of its simplicity and reliability. As for the single-end distance measurement methods, they are composed of time-domain approaches and industrial-frequency electrical component approaches [2,16,17].

In [18,19], fault distance can be obtained by solving nonlinear equations via eliminating double-end current and keeping the system parameters based on full network derivative equations. Several methods have been developed such as industrial-frequency impedance, fault location recertification method, and network hole equation and so on [10,18,19]. However, this kind of algorithms can not eliminate the impact of the variation of double terminal system impedance on the fault distance theoretically. One method of fault location considering the effect of capacitance to ground and distributed parameter of the

transmission line is applied in [20]. Hence an accurate fault distance can be acquired via the voltage and current values at the measurement terminal. The proposed algorithms possess high accuracy and robustness, but would not be affected by the fault resistance component.

A lot of successful practical applications for fault distance measurement based on traveling wave theory in the power transmission system have been developed [17,21–23].The system parameters, the variation of system operation modes, asymmetric electrical lines and transformer variation error and other factors have little impact on the method of traveling wave. However, there are still many key questions to be solved, *i.e.*, the determination of the traveling wave measurement pattern, the acquirement of the traveling wave signal, hybrid line and more-branch line.

During the procedure of fault analysis, the effect of the fault transient resistance can not be eliminated. Because of the centralized parameters of transmission line, neglecting the influence of distributed capacitor, could result in theoretical error in the fault distance calculation. Besides, the locomotive is a moving load, and it cannot be cut off from the operation immediately after the fault occurs. If this situation is omitted, the measurement error will be increased because of the effect of the fault transient resistance and locomotive current, and consequently the fault location estimation will fail.

Currently, in traction network system, the general used fault distance measurement method is impedance method, which can eliminate the influence of the fault transient resistance. However, the obtained fault distance from this method is only accurate under the condition of single-side power supply and without locomotive load. In this paper, methods for faut location in traction network system with single-phase short-circuit fault is proposed involving voltages and currents at the measurement terminal. The impact factors on the accuracy of fault distance location are also discussed, *i.e.*, fault transient resistance, locomotive, system parameters. A series of simulation experiments have been implemented to test the accuracy and robustness of the proposed algorithms.

The remainder of the paper is organized as follows. Section II describes the algorithms for the calculation of fault position with and without the locomotive consideration under fault stable state condition. Simulation experiments are implemented to prove the effectiveness of the proposed algorithm in section III. Conclusions and future works are given in Section IV.

2. The Algorithms of Fault Distance Measurement

2.1. The Algorithm of Fault Location Calculation without Locomotive Consideration

A short-circuited fault traction system is shown in Figure 1. The traction substation is equivalent to a power source E_s with impedance Z_s. The length of the traction line is l, m and n are the beginning point and terminal point of the traction line. f is the fault point, and the distance from the electrical substation to the fault position is l_f.

Transmission line equation can be used to describe the energy transferring in the traction network system through contact network and track loop. The equivalent circuit model of the faulted traction network system (described in Figure 1) is shown in Figure 3. The fault transient resistance at the fault point is R_f. Generally, locomotive can be regarded as a direct current source (empty load is infinitive) or certain impedance Z_t. In this part, locomotive is treated as a current source with infinitive impedance. Here, assume the electrical traction line parameters are uniformly distributed, where the per-unit-length

resistance, inductance and capacitance are, *i.e.*, R_0, L_0, C_0, respectively. The ground inductance G_0 is ignored in this case. The values of the transmission line parameters are shown in Table 1 [24].

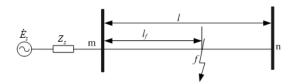**Figure 1.** The faulted traction network system.

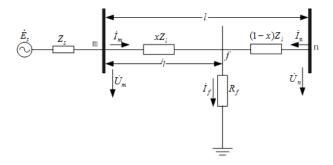**Table 1.** The electrical parameters of the traction line.

Parameter	Value
$R_0/(\Omega/\text{km})$	0.1–0.3
$L_0/(\text{mH/km})$	1.4–2.3
$C_0/(\text{nF/km})$	10–14

2.1.1. Lumped Transmission Line Parameter Condition

The short-circuit fault model with single-ended power supply and lumped transmission line parameters is shown in Figure 2. Z_l is the line impedance, and x is the per-unit-length from the measurement m-point to the fault, $x = \frac{l_f}{l}$. The voltage at the measurement m-point is expressed as,

$$\dot{U}_m = \dot{I}_m \cdot x \cdot Z_l + \dot{I}_f \cdot R_f \tag{1}$$

Figure 2. The faulted traction network system.

Since it is a open-circuit model, $\dot{I}_m = \dot{I}_f$, then $\dot{U}_m = \dot{I}_m \cdot x \cdot Z_l + \dot{I}_m \cdot R_f$. As the Equation (1) is a complex form, it can be derived into real part and imaginary part functions, therefore,

$$\text{Im}(\dot{U}_m) = \text{Im}(I_m Z_l) \cdot x + \text{Im}(\dot{I}_m) \cdot R_f \tag{2a}$$

$$\text{Re}(\dot{U}_m) = \text{Re}(I_m Z_l) \cdot x + \text{Re}(\dot{I}_m) \cdot R_f \tag{2b}$$

Multiply Equation (2a) by $\mathrm{Re}(\dot{I}_m)$ and Equation (2b) by $\mathrm{Im}(\dot{I}_m)$, and then subtract both side of the equations, it gives,

$$x = \frac{\mathrm{Re}(\dot{I}_m)\,\mathrm{Im}(\dot{U}_m) - \mathrm{Im}(\dot{I}_m)\,\mathrm{Re}(\dot{U}_m)}{\mathrm{Re}(\dot{I}_m)\,\mathrm{Im}(\dot{I}_m Z_l) - \mathrm{Im}(\dot{I}_m)\,\mathrm{Re}(\dot{I}_m Z_l)} \tag{3}$$

Based on the Equation (3), the fault location can be derived with the voltage and current at m-end measurement with the influence of fault resistance component R_f.

2.1.2. Distribution Transmission Line Parameter Condition

The propagation constant γ and characteristic impedance Z_c of the system parameters are,

$$\gamma = \sqrt{(R_0 + jwL_0)jwC_0}$$
$$Z_c = \sqrt{(R_0 + jwL_0)/jwC_0}$$

At the occurrence of short-circuit ground fault, based on the superposition principle, the system is composed of pre-fault and fault additional status [20], as shown in Figure 3(a) and Figure 3(b). As for the fault state variables, they can be obtained from the calculation from electrical measurements before and after the fault occurrence, then

$$\dot{U}_m^{(1)} = \dot{U}_m' + \dot{U}_m^{(0)}$$
$$\dot{I}_m^{(1)} = \dot{I}_m' + \dot{I}_m^{(0)} \tag{4}$$

where $\dot{U}_m'$ and $\dot{I}_m'$ are the voltage and current at m-point during fault time; $\dot{U}_m^{(1)}$ and $\dot{I}_m^{(1)}$ are the voltage and current values at m-point after fault occurrence; $\dot{U}_m^{(0)}$ and $\dot{I}_m^{(0)}$ are the voltage and current at m-point before fault occurring. Based on the fundamental transmission line equation [25], the voltage $\dot{U}_f'$ and current components $\dot{I}_f'$ at l_f fault point [see Figure 3(b)] are,

$$\dot{U}_f' = \dot{U}_m' \cosh \gamma l_f - \dot{I}_m' Z_c \sinh \gamma l_f$$
$$\dot{I}_f' = \dot{I}_m' \cosh \gamma l_f - \frac{\dot{U}_m'}{Z_c} \sinh \gamma l_f \tag{5}$$

where $cosh$ and $sinh$ are the hyperbolic curve functions. The fault component at n-end can be expressed as,

$$-\dot{I}_n' = (\dot{I}_f' - \dot{I}_f) \cosh \gamma(l - l_f) - \frac{\dot{U}_f'}{Z_c} \sinh \gamma(l - l_f) \tag{6}$$

Here, single substation power supply is applied. It is an open circuit at n-terminal, hence, $\dot{I}_n' = 0$. Then the fault current $\dot{I}_f'$ can be derived from Equations (5) and (6),

$$\dot{I}_f' = \frac{\dot{I}_m' \cosh \gamma l - \frac{\dot{U}_m'}{Z_c} \sinh \gamma l}{\cosh \gamma(l - l_f)} \tag{7}$$

Since the fault current $\dot{I}_f'$ is generated by the fault component, the post-fault current $\dot{I}_f = \dot{I}_f'$ [see Figure 3(a),3(b)]. Then the voltage at fault position after fault occurs can be described as:

$$\dot{U}_f = \dot{U}_m^{(1)} \cosh \gamma l_f - \dot{I}_m^{(1)} Z_c \sinh \gamma l_f \tag{8}$$

Therefore, the equivalent impedance Z_f at the fault point with Equations (7) and (8) is

$$Z_f = \frac{\dot{U}_f}{\dot{I}_f} = \frac{\dot{U}_f \cosh \gamma(l - l_f)}{C_m} = \frac{\dot{U}_f \cosh \gamma(l - l_f)\overline{C}_m}{|C_m|} \tag{9}$$

where $|C_m|$ and $\overline{C}_m$ are the modulus and conjugation of C_m; $C_m = \dot{I}'_m \cosh \gamma l - \frac{\dot{U}'_m}{Z_c} \sinh \gamma l$ without fault distance l_f. Generally, the short-circuit transient impedance Z_f is a pure resistance, it has
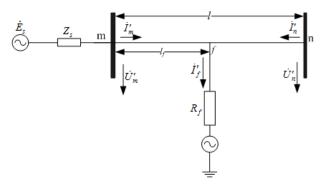
$$\mathrm{Im}(Z_f) = \mathrm{Im}\left(\frac{\dot{U}_f \cosh\gamma(l - l_f)\overline{C}_m}{|C_m|}\right) = 0$$
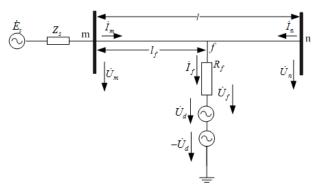
then

$$\mathrm{Im}\left(\dot{U}_f \cosh\gamma(l - l_f)\overline{C}_m\right) = 0 \tag{10}$$

where Im delegates the calculation of the imaginary part of the variable. From Equation (10), it can be seen that the equation has no relationship to the short-circuit fault transient resistance and system impedance considering the influence of system capacitor factors. With the knowledge of voltage and current at m position before and after the fault, the distance of the fault l_f can be located by solving the above equation, together with the electrical line parameters.

Figure 3. The equivalent model of faulted traction network system.

(a) The equivalent model after the fault occurrence

(b) The equivalent model during fault occurrence period

Figure 4. The relationship between the fault distance l_f and $F(l_f)$.

However, the direct solution from Equation (10) could bring a lot of calculating load. One way to solve this problem is to find the relationship between the fault distance and $F(l_f) = \text{Im}(\dot{U}_f cosh\gamma(l - l_f)\overline{C}_m)$, which is depicted in Figure 4. Through the relationship curve, the fault point can be located. However, the accuracy of the calculated fault distance is dependent on the precision of the curve. Another way to solve the problem is to simplify the equation. From Equation (10), it has

$$\text{Im}(\dot{U}_f cosh\gamma(l - l_f)\overline{C}_m) = \text{Im}(\dot{U}_f \overline{C}_m) \, \text{Re}(cosh\gamma(l - l_f)) \\ + \text{Re}(\dot{U}_f \overline{C}_m) \, \text{Im}\,(cosh\gamma(l - l_f)) \tag{11}$$

where Re calculation is to get the real part of the variable. Let $x = l - l_f$, then $x \in [0, l]$. Due to the small value of propagation coefficient γ and sufficiently short transmission line, the approximations are adopted,

$$\text{Re}(cosh\gamma x) \approx 1 \qquad \text{Im}(cosh\gamma x) \approx 0$$
$$\text{Re}(sinh\gamma x) \approx \text{Re}(\gamma x) \qquad \text{Im}(sinh\gamma x) \approx \text{Im}(\gamma x)$$

Hence, the Equation (11) can be simplified as

$$\text{Im}(\dot{U}_f cosh\gamma(l - l_f)\overline{C}_m) = \text{Im}(\dot{U}_f)Re(\overline{C}_m) + Re(\dot{U}_f)\text{Im}(\overline{C}_m) \tag{12}$$

And,

$$\text{Im}(\dot{U}_f) = \text{Im}(\dot{U}_m) - l_f \left(\text{Im}(\dot{I}_m Z_c)Re(\gamma) + \text{Re}(\dot{I}_m Zc) \, \text{Im}(\gamma) \right) \\ \text{Re}(\dot{U}_f) = \text{Re}(\dot{U}_m) - l_f \left(\text{Re}(\dot{I}_m Z_c) \, \text{Re}(\gamma) + \text{Im}(\dot{I}_m Z_c) \, \text{Im}(\gamma) \right) \tag{13}$$

Put Equations (12) and (13) into Equation (11), it has

$$\text{Im}(\dot{U}_f cosh\gamma(l - l_f)\overline{C}_m) = \left(\text{Im}(\dot{U}_m) - A \cdot l_f \right) \text{Re}(\overline{C}_m) \\ + \left(Re(\dot{U}_m) - B \cdot l_f \right) \text{Im}(\overline{C}_m) \tag{14}$$

where $A = \text{Im}(\dot{I}_m Z_c) Re(\gamma) + \text{Re}(\dot{I}_m Z_c) \text{Im}(\gamma)$, $B = \text{Re}(\dot{I}_m Z_c) Re(\gamma) - \text{Im}(\dot{I}_m Z_c) \text{Im}(\gamma)$. Therefore, l_f can be derived from Equations (10) and (14),

$$l_f = \frac{\text{Im}(\dot{U}_m) Re(\overline{C}_m) + Re(\dot{U}_m) \text{Im}(\overline{C}_m)}{Re(\overline{C}_m) A + \text{Im}(\overline{C}_m) B} \tag{15}$$

Therefore, Equation (15) is the calculation of fault location for traction network system. It can be demonstrated that the equation includes only the voltage and current at measurement point before and after the fault occurrence. The calculated fault distance l_f derived from the equation will not be affected by the transient resistance R_f, power source impedance Z_s and fault occurrence angle and other factors.

2.2. Fault Distance Measurement with the Consideration of Locomotive

The equivalent model of the short-circuit fault of the traction system is shown in Figure 5, t is the locomotive position and l_t is the distance between locomotive and electrical substation. In this case, the fault voltage and current components at locomotive position [see Figure 5(b)] and fault position can be described as,

$$\dot{U}'_f = \dot{U}'_t \cosh(\gamma(l_f - l_t)) - \dot{I}'_{t2} Z_c \sinh(\gamma(l_f - l_t)) \tag{16a}$$

$$\dot{I}'_{f1} = \dot{I}'_{t2} \cosh(\gamma(l_f - l_t)) - \frac{\dot{U}'_t}{Z_c} \sinh(\gamma(l_f - l_t)) \tag{16b}$$

$$\dot{U}'_t = \dot{U}'_m \cosh(\gamma l_t) - \dot{I}'_m Z_c \sinh(\gamma l_t) \tag{16c}$$

$$\dot{I}'_{t1} = \dot{I}'_m \cosh(\gamma l_t) - \frac{\dot{U}'_m}{Z_c} \sinh(\gamma l_t) \tag{16d}$$

where $\dot{U}'_f$, $\dot{I}'_{f1}$, $\dot{U}'_t$ and $\dot{I}'_{t1}$ are the voltage and current values at fault position and locomotive position respectively.

At the locomotive position, it has

$$\dot{I}'_{t2} = \dot{I}'_{t1} - \dot{I}'_t = \dot{I}'_{t1} - \frac{\dot{U}'_t}{Z_t}. \tag{17}$$

Put Equations (16c),(16d) and (17) into Equation (16a), and (16b), then

$$\begin{aligned}
\dot{U}'_f &= \dot{U}'_m[\cosh(\gamma l_f) + \tfrac{Z_c}{Z_t} \cosh(\gamma l_t) \sinh(\gamma(l_f - l_t))] \\
&\quad - \dot{I}'_m[Z_c \sinh(\gamma l_f) + \tfrac{Z_c^2}{Z_t} \sinh(\gamma l_t) \sinh(\gamma(l_f - l_t))] \\
\dot{I}'_{f1} &= \dot{I}'_m[\cosh(\gamma l_f) + \tfrac{Z_c}{Z_t} \sinh(\gamma l_t) \cosh(\gamma(l_f - l_t))] \\
&\quad - \tfrac{\dot{U}'_m}{Z_c}[\sinh(\gamma l_f) + \tfrac{Z_c}{Z_t} \cosh(\gamma l_t) \cosh(\gamma(l_f - l_t))]
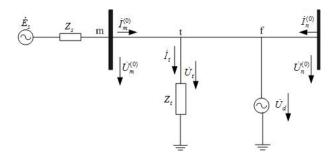\end{aligned} \tag{18}$$

The current at n-end is,

$$-\dot{I}'_n = (\dot{I}'_{f1} - I'_f) \cosh(\gamma(l - l_f)) - \frac{\dot{U}'_f}{Z_c} \sinh(\gamma(l - l_f)) \tag{19}$$
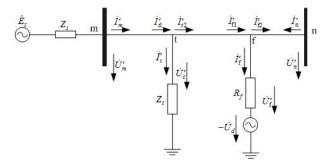
Since the circuit is open at n-end, therefore, $\dot{I}'_n = 0$, then $\dot{I}'_f$ is derived from Equation (19),

$$\dot{I}'_f = \frac{\dot{I}'_{f1} \cosh(\gamma(l - l_f)) - \frac{\dot{U}'_f}{Z_c} \sinh(\gamma(l - l_f))}{\cosh(\gamma(l - l_f))} \tag{20}$$
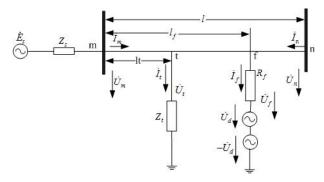
Figure 5. The equivalent model of faulted traction network system.

(a) The equivalent model of the pre-fault traction network system.

(b) The equivalent model during fault occurrence period.

(c) The equivalent model of the post-fault traction network system.

The current and voltage at the fault point in Figure 5(b) and 5(c) have the same values, *i.e.*, $\dot{I}'_f = \dot{I}_f$, $\dot{U}'_f = \dot{U}_f$. According to Equations (18) and (20),

$$\frac{\dot{U}_f}{\dot{I}_f} = \frac{\dot{U}_f \cosh(\gamma(l - l_f))}{C_m} \tag{21}$$

$$C_m = \dot{I}'_m[\cosh(\gamma l) + \frac{Z_c}{Z_t} \sinh(\gamma l_t) \cosh(\gamma(l - l_t))]$$
$$- \frac{\dot{U}'_m}{Z_c}[\sinh(\gamma l) + \frac{Z_c}{Z_t} \cosh(\gamma l_t) \cosh \gamma(l - l_t)]$$

Since the ground impedance is pure resistance, therefore, the imaginary part of $\frac{\dot{U}_f}{\dot{I}_f}$ is zero, then

$$\mathrm{Im}(\frac{\dot{U}_f}{\dot{I}_f}) = \mathrm{Im}(\frac{\dot{U}_f \cosh(\gamma(l - l_f))\overline{C}_m}{|\overline{C}_m|}) = 0 \tag{22}$$

Using the simplification of small value described in Section 2.1.2. and liberalization, then

$$\mathrm{Im}(\dot{U}_f)\mathrm{Re}(\overline{C}_m) + \mathrm{Re}(\dot{U}_f)\mathrm{Im}(\overline{C}_m) = 0 \tag{23}$$

and

$$\mathrm{Re}(\dot{U}_f) = \mathrm{Re}(\dot{U}_m) - l_f[\mathrm{Re}(\dot{I}_m Z_c)\mathrm{Re}(\gamma) - \mathrm{Im}(\dot{I}_m Z_c)\mathrm{Im}(\gamma)]$$
$$+ (l_f - l_t)[\mathrm{Re}(\dot{U}_m \tfrac{Z_c}{Z_t})\mathrm{Re}(\gamma) - \mathrm{Im}(\dot{U}_m \tfrac{Z_c}{Z_t})\mathrm{Im}(\gamma)]$$

$$\mathrm{Im}(\dot{U}_f) = \mathrm{Im}(\dot{U}_m) - l_f[\mathrm{Im}(\dot{I}_m Z_c)\mathrm{Re}(\gamma) + \mathrm{Re}(\dot{I}_m Z_c)\mathrm{Im}(\gamma)]$$
$$+ (l_f - l_t)[\mathrm{Im}(\dot{U}_m \tfrac{Z_c}{Z_t})\mathrm{Re}(\gamma) + \mathrm{Re}(\dot{U}_m \tfrac{Z_c}{Z_t})\mathrm{Im}(\gamma)]$$

After the same simplification during the calculation, the fault distance l_f can be derived as,

$$l_f = \frac{\mathrm{Im}(\dot{U}_m)\mathrm{Re}(\overline{C}_m) + \mathrm{Re}(\dot{U}_m)\mathrm{Im}(\overline{C}_m) - l_t A}{\mathrm{Re}(\overline{C}_m)B + \mathrm{Im}(\overline{C}_m)C} \tag{24}$$

where l_f is the calculated fault distance, and

$$A = [\mathrm{Im}(\dot{U}_m \tfrac{Z_c}{Z_t})\mathrm{Re}(\gamma) + \mathrm{Re}(\dot{U}_m \tfrac{Z_c}{Z_t})\mathrm{Im}(\gamma)]\mathrm{Re}(\overline{C}_m)$$
$$+ [\mathrm{Re}(\dot{U}_m \tfrac{Z_c}{Z_t})\mathrm{Re}(\gamma) - \mathrm{Im}(\dot{U}_m \tfrac{Z_c}{Z_t})\mathrm{Im}(\gamma)]\mathrm{Im}(\overline{C}_m)$$

$$B = \mathrm{Im}(\dot{I}_m Z_c)\mathrm{Re}(\gamma) + \mathrm{Re}(\dot{I}_m Z_c)\mathrm{Im}(\gamma) - \mathrm{Im}(\dot{U}_m \tfrac{Z_c}{Z_t})\mathrm{Re}(\gamma)$$
$$- \mathrm{Re}(\dot{U}_m \tfrac{Z_c}{Z_t})\mathrm{Im}(\gamma)$$

$$C = \mathrm{Re}(\dot{I}_m Z_c)\mathrm{Re}(\gamma) - \mathrm{Im}(\dot{I}_m Z_c)\mathrm{Im}(\gamma) - \mathrm{Re}(\dot{U}_m \tfrac{Z_c}{Z_t})\mathrm{Re}(\gamma)$$
$$+ \mathrm{Im}(\dot{U}_m \tfrac{Z_c}{Z_t})\mathrm{Im}(\gamma)$$

However, after a large amount of simulation experiments, it can be proved that the current value at locomotive point is quite small [shown in Equation (17)]. Therefore, the current at locomotive direction, $\dot{I}'_t$ can be ignored. In this case, the fault distance l_f can still be calculated with Equation (15). It also demonstrates that the position of locomotive has little impact on the fault point location. The proposed algorithms are tested by a series of simulation experiments.

2.3. The Algorithm of Fault Distance Measurement When Locomotive Is Regarded as a Constant Power Load

In this case, the locomotive is regarded as a constant power load. Figure 5 can still be used here for further analysis. Therefore, from Equation (17) at l_t point it has,

$$\dot{I}'_{t2} = \dot{I}'_{t1} - \frac{P}{\dot{U}'_t} = \dot{I}'_{t1} - D \tag{25}$$

where $D = \frac{P}{\dot{U}'_t}$ is a constant. The power of the locomotive P is known and the position of locomotive is known as well. Put Equations (16c), (16d) and (25) into Equations (16a), (16b),

$$\dot{U}'_f = \dot{U}'_m \cosh(\gamma l_f) - \dot{I}'_m Z_c \sinh(\gamma l_f) + A Z_c \sinh(\gamma(l_f - l_t)) \dot{I}'_{f1} = \dot{I}'_m \cosh\gamma l_f - \frac{\dot{U}'_m}{Z_c}\sinh(\gamma l_f) - A\cosh\gamma(l_f - l_t)$$
(26)

Still since the circuit is an open circuit, then

$$-\dot{I}'_n = (\dot{I}'_{f1} - \dot{I}'_f)\cosh(\gamma(l - l_f)) - \frac{\dot{U}'_f}{Z_c}\sinh(\gamma(l - l_f)) = 0$$
(27)

Using the same deduction steps described in Section 2.1.2., and the characteristics of the fault resistance, it has,

$$\mathrm{Im}(\frac{\dot{U}_f}{\dot{I}_f}) = \mathrm{Im}(\frac{\dot{U}_f \cosh\gamma(l - l_f)\overline{C}_m}{|\overline{C}_m|}) = 0$$
(28)

where $C_m = \dot{I}'_m \cosh(\gamma l) - \frac{\dot{U}'_m}{Z_c}\sinh(\gamma l) - A\cosh\gamma(l_f - l_t)$. The the calculation of fault distance l_f is,

$$l_f = \frac{\mathrm{Im}(\dot{U}_m)\mathrm{Re}(\overline{C}_m) + \mathrm{Re}(\dot{U}_m)\mathrm{Im}(\overline{C}_m) - l_t H}{\mathrm{Re}(\overline{C}_m)W + \mathrm{Im}(\overline{C}_m)S}$$
(29)

where

$$H = [\mathrm{Re}(AZ_c)\mathrm{Re}(\gamma) - \mathrm{Im}(AZ_c)\mathrm{Im}(\gamma)]\mathrm{Im}(\overline{C}_m)$$
$$+ [\mathrm{Im}(AZ_c)\mathrm{Re}(\gamma) + \mathrm{Re}(AZ_c)\mathrm{Im}(\gamma)]\mathrm{Re}(\overline{C}_m)$$

$$W = \mathrm{Im}(\dot{I}_m Z_c)\mathrm{Re}(\gamma) + \mathrm{Re}(\dot{I}_m Z_c)\mathrm{Im}(\gamma) - \mathrm{Im}(AZ_c)\mathrm{Re}(\gamma) - \mathrm{Re}(AZ_c)\mathrm{Im}(\gamma)$$

$$S = \mathrm{Re}(\dot{I}_m Z_c)\mathrm{Re}(\gamma) - \mathrm{Im}(\dot{I}_m Z_c)\mathrm{Im}(\gamma) - \mathrm{Re}(AZ_c)\mathrm{Re}(\gamma) + \mathrm{Im}(AZ_c)\mathrm{Im}(\gamma)$$

In this part, different algorithms of fault distance measurement are discussed under various conditions. Simulation experiments are implemented to discuss the accuracy of the proposed algorithms in different situations in the next section.

3. Simulation Results

The system described in Figure 1 is used for the following simulation experiments. Single-phase industrial-frequency AC power is supplied for the electrical traction system. Normally, the Electrical substation transform the 3-phase 110 kV high voltage into 27.5 kV voltage and assign the single-phase to each traction system. Therefore, in the experiments, the traction power sources $E_s = 27.5$ kV with impedance $Z_s = 0.245 + j1.055$. The traction line length l is 30 km. According to the transmission line parameters described in Table 1, the traction line parameters are $R_0 = 0.232$ Ω /km, $L_0 = 1.64$ mH/km, $C_0 = 10.5$ nF/km. The sampling frequency is 200 kHz, and the voltage sampling data of the first cycle are used as the input. Then Equations (3), (15), (24) and (29) are used to solve fault distance l_f, where the four fault distance estimation algorithms are delegated by **M1**, **M2**, **M3** and **M4** respectively.

The calculated fault distance can be evaluated through the comparison with the actual fault distance in the following equation,

$$e_{l_f} = \left| \frac{l_{f-calculated} - l_f}{l} \right|$$
(30)

where $l_{f-calculated}$ is the calculated fault distance from the developed algorithms and l_f is the actual fault point in the system.

Table 2 lists the results with three approaches: Reactance, Lumped parameter (**M1**) and Distributed parameter (**M2**) for fault distance calculation under various fault transient resistances and fault positions and zero load. It shows that the results derived from Reactance approach are the same as those derived from (**M1**). It is true since they share the same theory only with different calculation procedures. Compared the results from (**M1**) and (**M2**), the estimated fault distance from (**M2**) is more accurate since the transmission line characteristics are considered in the algorithms.

Table 2. The l_f estimation with different fault transient resistance R_f and $Z_t = \infty$.

R_f (Ω)	l_f (km)	Fault distance measurement and results					
		Reactance		Lumped para (M1)		Distributed para (M2)	
		Calculated	e_{l_f} (%)	Calculated	e_{l_f} (%)	Calculated	e_{l_f} (%)
0	6	5.9691	0.1030	5.9691	0.1030	6.0001	0.0003
	14	13.9288	0.2373	13.9288	0.2373	14.0013	0.0043
	26	25.8733	0.4223	25.8733	0.4223	26.0083	0.0277
50	6	5.4884	1.7053	5.4884	1.7053	6.0169	0.0563
	14	13.4355	1.8817	13.4355	1.8817	14.0258	0.0860
	26	25.3421	2.1930	25.3421	2.1930	26.0255	0.0850
100	6	4.0522	6.4927	4.0522	6.4927	6.03376	0.1125
	14	11.9867	6.7110	11.9867	6.7110	14.0503	0.1677
	26	23.8542	7.1527	23.8542	7.1527	26.0427	0.1423

The influence of the locomotive Z_t and fault transient resistance R_f when the fault distance is calculated from (**M3**) are discussed. Tables 3–6 demonstrate that the accuracy of $l_{f-calculated}$ is related to the magnitude of R_f, that is to say, the fault type. With the growing of the fault transient resistance, the fault distance algorithms (**M3**) could results in failure. However, the algorithm described in (**M2**) is not affected by the R_f, since the locomotive is not considered. Although better fault distance calculation can be obtained from algorithm of **M2** in ideal status, the effect of the locomotive in actual operational environment can not be omitted due to uncertain factors.

Table 3. The l_f estimation with various locomotive load when $l_t = 5$ km, $R_f = 0$ Ω.

| Locomotive load Z_t | Fault distance $l_f(km)$ | Fault distance measurement and results | | | |
| | | Reactance | | New algorithm (M3) | |
		Calculated	e_{l_f} (%)	Calculated	e_{l_f} (%)
	6	5.9600	0.1333	6.0473	0.1579
$Z_t = 54$	14	13.1838	2.7207	14.4146	1.3820
	26	21.8284	13.9052	26.9293	3.0978
	6	5.9609	0.1303	6.0424	0.1415
$Z_t = 60$	14	13.2589	2.4703	14.3728	1.2427
	26	22.2239	12.5870	26.8403	2.8012
	6	5.9616	0.1278	6.0384	0.1283
$Z_t = 66$	14	13.3204	2.2653	14.3387	1.1291
	26	22.5508	11.4973	26.7670	2.5567

Table 4. The l_f estimation with various locomotive load when $l_t = 5$ km, $R_f = 20$ Ω.

| Locomotive load Z_t | Fault distance $l_f(km)$ | Fault distance measurement and results | | | |
| | | Reactance | | New algorithm (M3) | |
		Calculated	e_{l_f} (%)	Calculated	e_{l_f} (%)
	6	5.4592	1.8027	6.0499	0.1666
$Z_t = 54$	14	9.4120	15.2930	14.564	1.8830
	26	14.4751	38.4163	27.2918	4.3060
	6	5.4868	1.7105	6.0445	0.1485
$Z_t = 60$	14	9.6849	14.3835	14.4936	1.6453
	26	15.1344	36.2185	27.1305	3.7683
	6	5.5112	1.6293	6.0405	0.1352
$Z_t = 66$	14	9.9272	13.5760	14.4385	1.4617
	26	15.7247	34.2510	27.0048	3.3493

Table 5. The l_f estimation with various locomotive load when $l_t = 5$ km, $R_f = 50\ \Omega$.

Locomotive load Z_t	Fault distance $l_f(km)$	Fault distance measurement and results			
		Reactance		New algorithm (M3)	
		Calculated	e_{l_f} (%)	Calculated	e_{l_f} (%)
	6	5.1116	2.9613	6.0540	0.1802
$Z_t = 54$	14	7.1568	22.8107	14.7998	2.6660
	26	9.9079	53.6401	27.8583	6.1944
	6	5.1260	2.9133	6.0478	0.1594
$Z_t = 60$	14	7.3888	22.0371	14.6809	2.2697
	26	10.4525	51.8250	27.5800	5.2667
	6	5.1394	2.8684	6.0437	0.1460
$Z_t = 66$	14	7.6073	21.3089	14.5921	1.9738
	26	10.9677	50.1077	27.3710	4.5700

Table 6. The l_f estimation with various locomotive load when $l_t = 5$ km, $R_f = 100\ \Omega$.

Locomotive load Z_t	Fault distance $l_f(km)$	Fault distance measurement and results			
		Reactance		New algorithm (M3)	
		Calculated	e_{l_f}(%)	Calculated	e_{l_f} (%)
	6	4.8602	3.7990	6.0613	0.2043
$Z_t = 54$	14	5.8106	27.2978	15.2187	4.0625
	26	7.1359	62.8801	28.868	9.5600
	6	4.8440	3.8533	6.0535	0.1785
$Z_t = 60$	14	5.9320	26.8932	15.0100	3.3667
	26	7.4535	61.8215	28.3701	7.9003
	6	4.8279	3.9069	6.0493	0.1646
$Z_t = 66$	14	6.0521	26.4929	14.8594	2.8647
	26	7.7684	60.7720	28.0080	6.6936

In Table 7, the fault distance is estimated when the locomotive is regarded as a constant power load. When the fault transient resistance is 0, the obtained fault distance from **M4** is more accurate. However, if the fault transient resistance R_f is increasing, the accuracy of the calculated fault distance will decrease gradually.

Table 7. The l_f calculation when locomotive is a constant power load.

Transient resistance $R_f(\Omega)$	Fault distance $l_f(km)$	Fault distance measurement and results			
		Reactance		New algorithm (M4)	
		Calculated	$e_{l_f}(\%)$	Calculated	$e_{l_f}(\%)$
0	6	5.9690	0.1030	5.8899	0.3670
	14	13.3714	2.0953	14.0058	0.0193
	26	22.2777	12.4077	25.7049	0.0193
50	6	4.7854	4.0487	6.66124	2.2010
	14	11.5264	8.2453	15.2937	4.3123
	26	19.4371	21.8763	27.3500	4.5000
100	6	3.7350	7.5500	7.6162	5.3873
	14	9.9142	13.6193	16.8078	9.3593
	26	16.9867	30.0443	29.2622	10.8740

It has to be noted that the simulation experimental results above are all obtained in ideal test environments. We have to admit there is no field experimented the paper due to test condition constraints. In actual fault distance measurement for electrical traction systems, there are many factors that could result in the failure of fault location detection, such as the fault transient resistance and the fluctuations in the electrical line parameters. If the correct fault position cannot be obtained via the current used fault location algorithm, other algorithms pre-programmed embedded in the measurement device can be used as alternatives to provide more estimation results so that at least one estimated fault position will close to the actual fault location. Besides, if more fault estimation algorithms are applied, different results could be used for the comparison to increase the precision of the estimated fault location. Therefore, to improve the accuracy of the fault position, other measurement methods should also be adopted, and the fault distance estimations should be compared considering the actual complicated operational environment.

4. Conclusions

In this paper, several algorithms of fault distance estimation are discussed based on the fault stable state characteristics in single-end direct power supply electrical traction system. The proposed algorithms in the paper are quite simple and can be easily applied. The fault distance can be deduced with the knowledge of voltages and currents at the measurement terminal of transmission line. Besides, compared to the traditional impedance method, the developed algorithms consider the factors of locomotive and fault transient resistance. Simulation results of the estimated fault distance location are quite accurate. However, measurement errors could inevitable happen when fault distance is estimated on the spot because of many uncontrollable factors such as worse weather conditions and wire aging. To improve the accuracy of the fault position, therefore, other measurement methods should be aided to compare the estimated fault distance considering the actual complicated operational environment.

Acknowledgments

References

1. Ekici, S. Support vector machines for classification and locating faults on transmission lines. *Appl. Soft Comput.* **2012**, *12*, 1650–1658.
2. Robert, S.; Stanislaw, O. Accurate fault location in the power transmission line using support vector machine approach. *IEEE Trans. Power Syst.* **2004**, *19*, 979–986.
3. De Morais Pereira, C.E.; Zanetta, L.C., Jr. An optimisation approach for fault location in transmission lines using one terminal data. *Int. J. Electr. Power Energy Syst.* **2007**, *29*, 290–296.
4. Takagi, T.; Yamakoshi, Y.; Yamaura, M. Development of a new type fault locator using the one-terminal voltage and current data. *IEEE Trans. PAS* **1982**, *101*, 2892–2898.
5. Waikar, D.L.; Chin, P.S.M. Fast and accurate parameter estimation algorithm for digital distance relaying. *Electr. Power Syst. Res.* **1998**, *44*, 53–60.
6. Zivanovic, R. An application of global sensitivity analysis in evaluation of transmission line fault-locating algorithms. *Procedia Soc. Behav. Sci.* **2010**, *2*, 7780–7781.
7. Avdakovic, S.; Nubanovic, A.; Kusljugic, M.; Kusljugicb, M.; Musica, M. Wavelet transform applications in power system dynamics. *Electr. Power Syst. Res.* **2012**, *83*, 237–245.
8. Bernadi, A.; Leonowicz, Z. Fault location in power networks with mixed feeders using the complex space-phasor and hilbert-huang transform. *Electr. Power Energy Syst.* **2012**, *42*, 208–219.
9. Jung, H.; Park, Y.; Han, M.; Leea, C.; Parka, H.; Shinb, M. Novel technique for fault location estimation on parallel transmission lines using wavelet. *Electr. Power Energy Syst.* **2007**, *29*, 76–82.
10. Firouzjah, K.G.; Sheikholeslami, A. A current independent method based on synchronized voltage measurement for fault location on transmission lines. *Simul. Model. Pract. Theory* **2009**, *17*, 692–707.
11. Guobing, S.; Jiale, S.; Ge, Y. An accurate fault location algorithm for parallel transmission lines using one-terminal data. *Electr. Power Energy Syst.* **2009**, *31*, 124–129.
12. Liao, Y. Transmission line fault location algorithms without requiring Line parameters. *Electr. Power Compon. Syst.* **2008**, *36*, 1218–1225.
13. Lin, X.; Weng, H.; Wang, B. A generalized method to improve the location accuracy of the single-ended sampled data and lumped parameter model based fault locators. *Electr. Power Energy Syst.* **2009**, *31*, 201–205.
14. Funk, A.T.; Malik, O.P. Impedance estimation including ground fault resistance error correction for distance protection. *Electr. Power Energy Syst.* **2000**, *22*, 59–66.
15. Jiale, S.; Qi, J. An accurate fault location algorithm for transmission line based on R-L model parameter identification. *Electr. Power Syst. Res.* **2005**, *76*, 17–24.

16. Lian, B.; Salama, M.M.A.; Chikhani, A.Y. A time domain differential equation approach using distributed parameter line model for transmission line fault location algorithm. *Electr. Power Syst. Res.* **1998**, *46*, 1–10.

17. Mardiana, R.; Motairy, H.A.; Su, C.Q. Ground fault location on a transmission line using high-frequency transient voltages. *IEEE Trans. Power Deliv.* **2011**, *26*, 1298–1299.

18. Jiale, S.; Guobing, S.; Xu, Q.; Chao, Q. Time-domain fault location algorithm for parallel transmission lines using unsynchronized currents. *Electr. Power Energy Syst.* **2006**, *28*, 253–260.

19. Jiang, Z.; Miao, S.; Xu, H.; Liu, P.; Zhang, B. An effective fault location technique for transmission grids using phasor measurement units. *Electr. Power Energy Syst.* **2012**, *42*, 653–660.

20. Cheng, W.; Xu, G.; Mu, L. A novel fault location algorithm for traction network based on distributed parameter line model. *Proc. CSU-EPSA* **2005**, *17*, 63–66.

21. Borghetti, A.; Corsi, S.; Nucci, C.A.; Paolone, M.; Peretto, L.; Tinarelli, R. On the use of continuous-wavelet transform for fault location in distribution power systems. *Electr. Power Energy Syst.* **2006**, *28*, 608–617.

22. Fan, C.; Li, K.K.; Chan, W.L.; Yu, W.; Zhang, Z. Application of wavelet fuzzy neural network in locating single line to ground fault in distribution lines. *Electr. Power Energy Syst.* **2007**, *29*, 497–503.

23. Ngu, E.E.; Ramar, K. A combined impedance and traveling wave based fault location method for multi-terminal transmission lines. *Electr. Power Energy Syst.* **2011**, *33*, 1767–1775.

24. Mariscotti, A.; Pozzobon, P. Synthesis of line impedance expressions for railway traction systems. *IEEE Trans. Vehicular Technol.* **2003**, *52*, 420–430.

25. Qiu, G. *Theory of Circuit*, 5th ed.; The Advaced Education Publisher: Xi'an, China, 2006.